

Link Cost Function and Link Capacity for Mixed Traffic Networks

Aathira K. Das¹ and Bhargava Rama Chilukuri¹

Transportation Research Record
2020, Vol. 2674(9) 38–50
© National Academy of Sciences:
Transportation Research Board 2020
Article reuse guidelines:
sagepub.com/journals-permissions
DOI: 10.1177/0361198120926454
journals.sagepub.com/home/trr



Abstract

Link cost function and link capacity are critical factors in traffic assignment modeling. Popular link cost functions like the Bureau of Public Roads (BPR) function have well-known drawbacks and are not suitable for mixed traffic conditions where a variety of vehicle classes use the road in a non-lane-based movement. Similarly, capacity is generally considered as a constant value. However, in mixed traffic conditions, capacity is not constant, but a function of vehicle class composition. Toward addressing these issues, this paper proposes a link cost function in relation to link travel time and link capacity in relation to vehicular traffic flow for mixed traffic conditions. The functions are developed based on the kinematic wave model, which is popularly used for estimating traffic dynamics on the roads. The developed link cost function and link capacity use field measurable parameters that incorporate mixed traffic features. The functions are validated against empirical data obtained from 12 signal cycles from two different signalized intersections in Chennai, India, representing different scenarios of mixed traffic, and it was found that the results match well with the empirical data.

Mixed traffic networks in developing countries comprise motorized and non-motorized vehicles with varying types, size, engine power, maneuverability, and so forth, and do not follow a lane-based movement. Some of the vehicle classes observed in mixed traffic networks include motorized two-wheelers, three-wheelers, four-wheelers, bicycles, light commercial vehicles (LCV), heavy commercial vehicles (HCV), and so forth. The vehicle characteristics combined with inter- and intra-vehicular interactions result in a broad range of speeds observed on these networks. The slow-moving vehicles such as buses and heavy vehicles occupy the lower ranges of the speeds, whereas the fast-moving cars and bikes dominate the higher ranges. Also, the bikes with their smaller size, higher speed, and ease of maneuverability easily move through the smaller available gaps in the traffic stream, giving rise to higher bike flows compared with that for the rest of vehicle classes in the traffic stream. Finally, lane-free movement of vehicles increases the complexity, owing to an extra degree of freedom for vehicular movement. Thus, the traffic flow, composition of vehicle classes, and traffic characteristics vary significantly across time and space in these networks. This mixture of different vehicle classes and non-lane-based movement causes complex traffic conditions on the

roads, which distinguish its combined flow behavior from that of a homogeneous flow (1). Thus, the traditional analysis tools and methods may need to be revisited to address the challenges posed by the mixed traffic networks.

Link cost function and link capacity play a vital role in transportation planning applications. To compute the link flows, link-specific cost function and link capacity are among the inputs required in traffic assignment problems (2). The link cost function is the relationship between the mean travel time and traffic flow on the links of urban networks. A typical link cost function should consider free-flow travel time on the link, link delay, and delay at intersections. There are several link cost functions and delay models popularly used for homogeneous traffic conditions, but because of their unique characteristics, they may not be suitable for mixed traffic. Similarly, link capacity is defined as the maximum allowable vehicular traffic flow under

¹Civil Engineering Department, Indian Institute of Technology Madras, Chennai, India

Corresponding Author:

Aathira K. Das, aathirakdas01@gmail.com

steady-state conditions. Generally, a constant value of link capacity is considered in traffic assignment problems. But, in mixed traffic conditions, the capacity is not a constant value but is a function of vehicular composition; for example, the higher the proportion of smaller or faster vehicles, the higher the flow. Also, the capacity of a link is a function of downstream control characteristics. If the link is always free-flowing, the mid-block capacity can be treated as the capacity of the link; however, if there is some downstream restriction to traffic flow, for example, because of geometry or a traffic signal, the characteristics of restriction drive the capacity of the link. Therefore, it is important to incorporate these features into the link cost and capacity function to replicate field conditions.

Literature Review

This section discusses the state-of-the-art research in the areas of link cost functions, link capacity, and traffic assignment in networks with mixed traffic flow. Furthermore, the research gaps are identified, and the contributions of this study to overcome them are briefly discussed.

Link Cost Function and Link Capacity

Some of the popular link cost functions used in the literature and practice include the Bureau of Public Roads (BPR) function, Davidson's function, the Akcelik function, and conical delay function (3). Among all these, BPR function, shown in Equation 1, is most commonly used.

$$t = t_0 \left(1 + \alpha \left(\frac{x}{C} \right)^\beta \right) \quad (1)$$

Here, t , t_0 , x , and C are the travel time, free-flow travel time, flow, and link capacity, respectively, and α and β are constant coefficients. It is a polynomial function, whose coefficients need to be calibrated using empirical data (4). Generally, 0.15 and 4 are used for α and β , respectively (2). Simple mathematical form, fewer and easily field-observable inputs, and reasonable performance are some of the reasons for its popular acceptance (5). However, it is evident from studies conducted subsequently that this function also has its drawbacks. The derivation of function does not take into account all the characteristics of traffic facility such as control at the intersection and the current operating condition (6). Boyce et al. noted that there is no parameter in the BPR function to account for different types of roadway facilities or different types of traffic operations (7). Skabardonis et al. also noted that the function overpredicts the average speed for $v/c > 1$ (6). The capacity is not

clearly defined in the BPR function, which can lead to unfeasible overflow on links. As a result, the equilibrium solution can have oversaturated links (7–10). Branston reviewed different link functions and observed that the flow on the link does not exceed the steady-state capacity, which is uniquely defined (11). Thus, Manzo argued that the BPR formula may be suitable only when the traffic flow is below capacity (12). For the links with flow far below the capacity, especially when the values of α are very high, the function always yields free-flow times independent of the actual flow on the link (8, 9). It was observed that the Davidson function rapidly increased the travel time as flow approached capacity and limits the flow to capacity, and it also resulted in unrealistically higher link travel times than the BPR equation (10). Conical volume delay function was developed as an alternative to BPR type functions (11). Though it could overcome the shortcomings of the BPR function, it was difficult to estimate the parameters. Rose et al. observed that the estimation of parameters of the BPR function is highly influenced by the rational determination of link capacity (13). Also, they noted that none of the variations of the BPR function can describe the characteristics of mixed traffic. Thus, it is evident that the traditional link cost functions are not suitable for mixed traffic networks.

It is important to note that, as mentioned earlier, intersection delay cost because of signal settings is an important component of the link cost function, which the traditional BPR function does not take into consideration. Several researchers have investigated the effect of signal delay on the performance of traffic assignment models. Aashtiani and Iravani used a simple delay function which was based on the first term of Webster's delay model and showed that the assignment flows improved (14). Jeihani et al. also showed that the prediction accuracy of traffic assignment models can be improved by including the intersection delays (15). Some researchers have used the popular Highway Capacity Manual (HCM) delay equation for intersection delay calculation, which is given as (16–18):

$$\begin{aligned} \text{Delay} = & \frac{C}{2} \times \frac{\left(1 - \frac{g}{c}\right)^2}{1 - \min\left(1, \frac{v}{c}\right) \times \frac{g}{C}} \\ & + \left((X - 1) + \sqrt{(X - 1)^2 + \frac{8klX}{cT}} \right) \end{aligned} \quad (2)$$

In Equation 2, the delay is in second/vehicle, C is the cycle length in seconds, c is the capacity, v is the vehicle arrival rate, X is the saturation flow rate or departing rate of vehicles, v/c is the degree of saturation, k is incremental delay factor, T is the analysis period, l is the

upstream filtering factor, and g/C is the effective green ratio for an approach. Horowitz compared the performance of the delay functions in HCM 1985 and HCM 1994 for traffic assignment models and found that both functions produced the same results (16). He concluded that a small modification in the BPR function cannot replace the delay calculation based on HCM or existing traffic flow theories. Kurth et al. also implemented HCM capacity and delay calculations into link travel time estimation which was found to produce reasonable traffic volumes under homogeneous traffic conditions (17). However, Koutsopoulos et al. considered dynamic intersection delay along with link delays based on procedures for intersection analysis from the HCM 1985 which were found to be suitable for small- and medium-scale networks (18). It led to a more realistic assignment but the calculations were time-consuming.

Link capacity is another important input for the traffic assignment models. As stated earlier, several studies have shown that the BPR function can lead to unfeasible overflow on links (7–10). When link flows exceed the link capacity, this leads to spillback to the upstream links which can be challenging to model. To overcome this issue, the capacity constraint was introduced in traffic assignment problems, imposing upper bounds on the link flows (10). Traffic flow on a link is restricted to the steady-state capacity of that link, which is defined as the “the capacity of the point providing poorest service on that link” (12). In almost all the studies in the literature, the capacity value for the BPR function is taken as a constant value, as defined by the mid-block capacity in the Highway Capacity Manual (19).

Traffic Assignment Models for Mixed Traffic

In the early decades, some of the studies focused on traffic assignment modeling in the mixed transportation network. Dafermos developed an algorithm for a multi-class user transportation network in which each class of vehicle has individual cost function without considering the interaction between the different vehicle classes on a link, and the problem is reduced into a single class user model (20). Later, Lam et al. presented a combined trip distribution and assignment model for a network with multiple user classes (21). The BPR function is used in the traffic assignment model to determine the travel time on links with the assumption that the free-flow travel time of all types of vehicles is identical for a link. Zhu et al. proposed a mixed traffic equilibrium model with the logit-based integrating mode, route, and transfer station choices (22). They studied the traveling choice behaviors under the influence of the cost, time, and user preferences. In this study, the actual travel cost is formulated as a weighted sum of all costs related to that single or combined mode using the BPR function. Mesbah et al.

proposed a non-linear integer programming model to optimize transit road space priority at the network level by minimizing the total travel time (23). A bi-level programming approach including logit mode-choice model and traffic assignment is employed to find the optimal combination of exclusive lanes for buses using the BPR function as the cost function.

As can be seen from the literature, the BPR function only represents the free-flow travel time on the link and link delay. To incorporate intersection delay, some of the studies used HCM delay models for homogeneous traffic conditions. But both these models use only one variable, the flow, to characterize the travel time. However, the travel time in the mixed traffic conditions depends not only on the flow but also depends on several other factors such as the vehicle class composition, their interactions, and the resulting traffic state. But, neither the BPR function nor the HCM delay model explicitly incorporates these heterogeneous flow characteristics to make them suitable for mixed traffic networks.

Also, the concept of a constant value for capacity does not apply to mixed traffic networks, since the capacity is dependent on the vehicle class composition. Further, in a signalized network, since the spillback from downstream intersection makes the modeling challenging, it may be more appropriate to set upper bounds on the capacity based on downstream traffic signal settings.

In light of these observed shortcomings, this paper proposes a link cost function and a link capacity incorporating the features of mixed traffic networks. The link cost function includes both link delay and intersection delay into one closed-form expression. Also, the link capacity, defined as the highest flow allowed on a link that does not result in a spillback to upstream intersections, is represented as a closed-form expression of the mixed traffic characteristics and signal settings. One of the main features of these functions is that all the parameters have a physical meaning and are easily field-observable/measurable.

The remainder of this paper is organized as follows: the next two sections explain the development of proposed link cost function and link capacity, which is the main contribution of this paper. Succeeding sections explain the data collection and analysis procedure for the evaluation of the developed functions against the traditional models. The last section discusses the key observations and inferences from this work.

Development of the Proposed Models

Link Cost Function

The new link cost function developed in this study has two parts; travel time on the link and the average delay

at the signalized intersection as shown in Equation 3.

$$T_{total} = T_{link} + D_{int} \quad (3)$$

where

T_{total} = total travel time on link

T_{link} = link travel time

D_{int} = average delay at the signalized intersection

To derive these two parts, the concept introduced by Das and Chilukuri is modified to include field-observable traffic flow parameters, as described in the following paragraphs (24).

Link Travel Time (T_{link})

The travel time on a link is defined as the time taken to traverse the link at steady-state traffic flow, q . If the steady-state relationship between speed and flow (also known as the fundamental diagram in traffic literature) on a link of the network is given by $u_q = f(q)$, then the speed for any flow can be found, and the travel time for the link of length L is given as:

$$T_{link} = \frac{L}{u_q} \quad (4)$$

Note that $f(q)$ may be unique for a given location and composition.

Intersection Delay (T_{delay})

To capture the features of real-world mixed traffic conditions, the shock wave analysis involving the parameters of a generic polynomial fundamental diagram used by Das and Chilukuri is considered in this study (24). The shockwave analysis gives a solution to the Lighthill-Whitham-Richards (LWR) model to estimate the congestion dynamics on

corridors (25). Shocks are formed in traffic streams when different traffic states interact.

Consider a road where traffic flow q is represented by the state A (q_A) (see Figure 1). Assume a traffic signal at the downstream intersection with a cycle length of C and red duration r . When the signal turns red, the traffic approaching the intersection will begin to slow down and stop at the stop line resulting in traffic state B . The flow rate in state B is zero, complying with the stop condition. This causes a backward-propagating shock wave s between traffic states A and B . According to the Rankine Hugoniot jump condition, the equation of shockwave speed s is written as shown in Equation 5 where k_J is the jam density (25).

$$s = \frac{q_A u_q}{k_J u_q - q_A} \quad (5)$$

When the signal turns green, backward-propagating wave ω is generated as the vehicles begin to discharge with traffic state C . The speed of the second wave will be higher as vehicles discharge at saturation flow, and the two waves would eventually meet at a point. This point signifies the maximum extent of queue spillback because of the red signal duration. Once the last vehicle in the queue is discharged, the traffic state changes back to A from C , characterized by a forward-propagating shock wave with a wave speed of u_{cr} . This process is depicted in Figure 1b More details of shock wave analysis can be found in May (25).

Let l be the length of the resulting queue at the intersection. Here, l is determined using the fundamental diagram and the shockwave diagram. From the shockwave diagram (Figure 1b), the length of the queue, l can be written as shown in Equation 6.

$$l = \frac{r s \omega}{\omega - s} \quad (6)$$

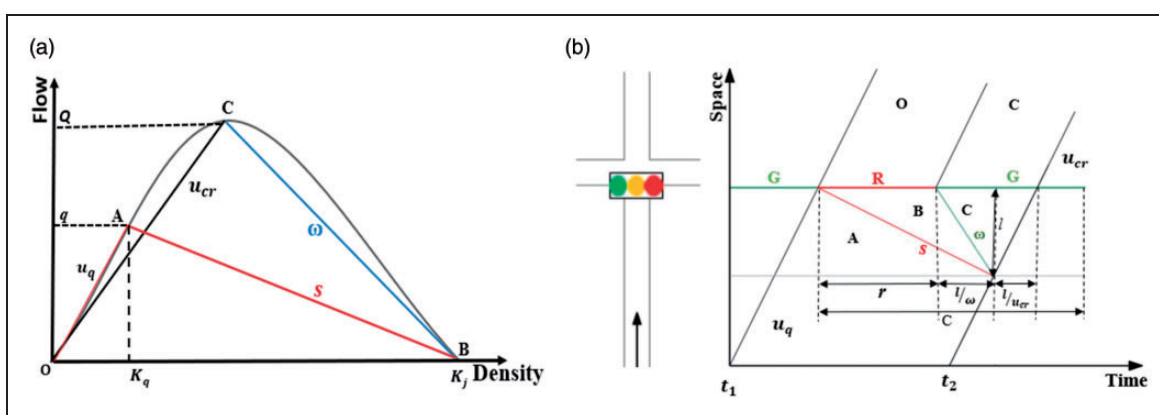


Figure 1. Delay calculation at the signalized intersection from: (a) fundamental diagram and (b) shockwave diagram.

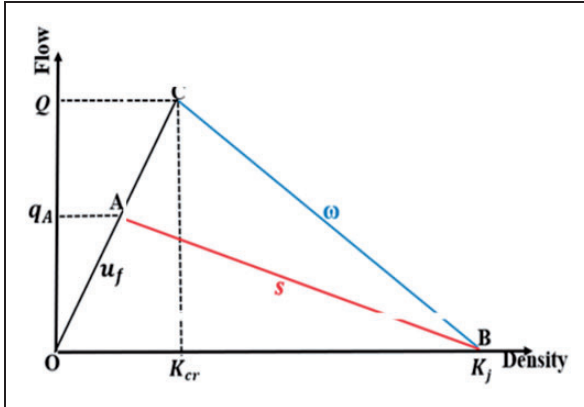


Figure 2. Triangular fundamental diagram with shockwaves formed at a signalized intersection.

Solving Equations 5 and 6, the expression for queue length, l , can be obtained, as shown in Equation 7.

$$l = \frac{ru_q q_A \omega}{\omega(k_j u_q - q_A) - u_q q_A} \quad (7)$$

The different states of flow and the parameters for delay calculation are shown in the time-space diagram (see Figure 1).

Delay at the signalized intersection is defined as the average delay experienced by all the vehicles impacted by the red duration. The effect of the red phase is felt by all the vehicles that join the queue during the period $T = t_2 - t_1$, as shown in Figure 1b. This, in turn, is equal to $\frac{l}{u_{cr}} + r + \frac{l}{\omega}$ where l is the queue length, u_{cr} is the critical speed, r is the red duration, and ω is the wave speed. During the red interval, the average delay incurred by a vehicle is $r/2$, whereas, during the green, the average delay is zero. Therefore, during the entire cycle, the average delay incurred by a vehicle at the signalized intersection is the weighted average of delay caused during the red and green phases. Therefore, for flow q_A the delay is given as,

$$D_{int} = \frac{(T * \frac{r}{2})}{c} = \frac{\frac{l}{u_{cr}} + r + \frac{l}{\omega}}{c} * \frac{r}{2} \quad (8)$$

Using Equations 4 and 8, total travel time on a link is obtained as in Equation 9.

$$T_{total} = \frac{L}{u_q} + \frac{\frac{l}{u_{cr}} + r + \frac{l}{\omega}}{c} * \frac{r}{2} \quad (9)$$

Therefore, this expression for the length of queue (Equation 7) formed on a link because of the red signal will be an input in the link cost function (Equation 9) to

determine the total travel time on the link. The fundamental diagram parameters u_{cr} , k_J , and ω , present in the equation reflect the mixed traffic characteristics on the link, and the red duration, r , represents the effect of the signal settings on the intersection delay. Note that the fundamental diagram parameters are a function of traffic composition and may vary by place.

In case the fundamental diagram is assumed to be triangular as shown in Figure 2, it will alter the shock-wave speeds, and Equation 9 will change (25). On the onset of green, the queue dissipates at saturation flow rate characterized by a forward-propagating shock wave with a wave speed equal to the free-flow speed u_f (instead of u_{cr}). Also, the stream speed will be u_f instead of u_q .

Thus, the link cost function given in Equation 9 will become:

$$T_{total} = \frac{L}{u_f} + \frac{\frac{l}{u_f} + r + \frac{l}{\omega}}{C} * \frac{r}{2} \quad (10)$$

where the queue length given by Equation 7 will become:

$$l = \frac{ru_f q_A \omega}{\omega(k_j u_f - q_A) - u_f q_A} \quad (11)$$

Using the relationship in Figure 2, the saturation flow Q of the link can be derived as given in Equation 12.

$$Q = \frac{k_j u_f \omega}{(u_f + \omega)} \quad (12)$$

Using 11 and 12 in 10,

$$T_{total} = \frac{L}{u_f} + \frac{r^2}{2c \left(1 - \frac{q_A}{Q}\right)} \quad (13)$$

Thus, with a triangular fundamental diagram, the proposed link cost function reduces to a function of only three parameters (r , $\frac{L}{u_f}$, $\frac{q_A}{Q}$) and is devoid of any other fundamental diagram parameters.

Figure 3 shows the behavior of the link intersection delay, the second term given in Equation 13 when plotted against the flow ratio, q_A/Q , for different values of r/C ratio. Note that since r will have a constant value, the plot only shifts vertically when multiplied with r , but the shape stays the same.

It can be observed that the link cost increases non-linearly with increasing $\frac{q_A}{Q}$. Also, the link cost function increases non-linearly with increasing r/C ratio for a given $\frac{q_A}{Q}$ value. When the demand flow q_A is smaller than the saturation flow (up to $\frac{q_A}{Q} = 0.6$), the slope of the curve changes marginally, but increases at a steeper

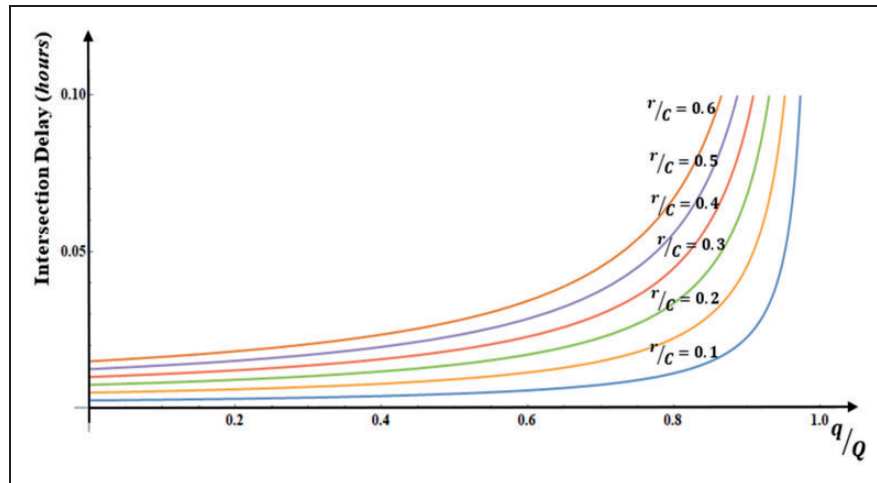


Figure 3. Sensitivity of link cost function to red ratio and flow ratio ($r = 0.05 \text{ h}$).

rate when demand approaches capacity. Note that the range of link cost values on the Y -axis of the graph will change with varying values of fundamental diagram parameters and red duration.

Link Capacity

In the context of this study, the link capacity is defined as the maximum flow allowed on a link that limits the queue spillback (because of red signal) within the link. Thus, each link and the corresponding downstream intersection act as an independent building block of the traffic network, not influenced by traffic conditions in the downstream link.

Based on this rationalization, the expression for link capacity (see Equation 14) is obtained from the equation for queue length (Equation 7) by replacing l with the link length L and flow q_A for link capacity C .

$$C = \frac{L\omega k_J u_q}{r u_q \omega + L(u_q + \omega)} \quad (14)$$

Note that link capacity is a function of link length, fundamental diagram parameters, and the red duration. Note that, when $r=0$ in Equation 14, it reduces to mid-block capacity given in Equation 12.

If the fundamental diagram is triangular, and when both numerator and denominator are divided by r , the link capacity function reduces to a function of only three parameters; k_J , $\frac{k_J}{Q}$, and $\frac{L}{r}$. Although these ratios do not have a physical meaning, a simple ratio of these parameters is sufficient to describe the behavior of this function, as shown below:

$$C = \frac{L\omega k_J u_f}{r u_f \omega + L(u_f + \omega)} = \frac{\left(\frac{L}{r}\right)k_J}{1 + \frac{L}{r} \left(\frac{k_J}{Q}\right)} \quad (15)$$

Figure 4 shows the behavior of the link capacity (Equation 15) when plotted against the L/r ratio, for different values of $\frac{k_J}{Q}$ ratio. Note that since k_J will have a constant value, the plot only shifts vertically when multiplied with k_J but the shape stays the same.

It is observed that the link capacity non-linearly increases with an increasing L/r ratio. However, as the L/r ratio increases ($r \rightarrow 0$), the cost asymptotically reaches the mid-block capacity (no traffic signal control). With an increase in $\frac{k_J}{Q}$ ratio, the link capacity decreases because of the decreasing saturation flow value. Note that the range of link capacity values on the Y -axis of the graph will change with varying values of fundamental diagram parameters and red duration.

The link cost and capacity function derived in Equations 9 and 14 are validated using empirical data, as described in the next section.

Data Collection and Analysis

Traffic Composition and Signal Settings

Two locations along Rajiv Gandhi Salai, a major state highway in Chennai, India, were identified for obtaining the empirical data for the validation of proposed functions. It is a 45 km long major state highway connecting Chennai City and Mahabalipuram, with large traffic volumes. Traffic data is collected from an approach of each of the signalized intersections. The first approach is a three-lane 150 m long link that terminates at the TIDEL Park intersection (see Figure 5). This intersection is situated near the TIDEL Park, which is a home for many major IT companies and is connected by East Coast Road on the east. The second approach is a three-lane 130 m long link that terminates at the CSIR intersection (see Figure 6). The reference line (AA')

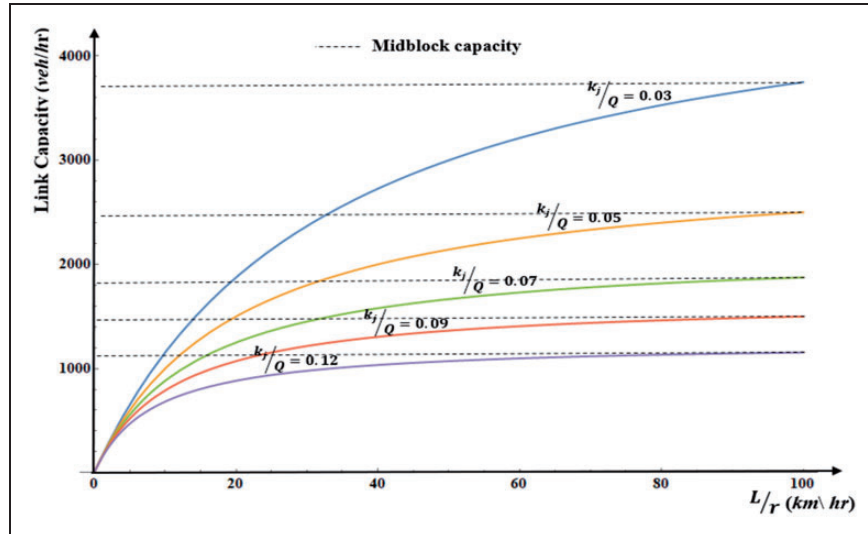


Figure 4. Sensitivity of link capacity to the ratio of link length and red time and ratio of jam density and saturation flow ($k_J = 150$ veh/km).



Figure 5. Study approach at the TIDEL Park intersection, Chennai, India.

marked is the halt line where the vehicles start moving on the onset of the green signal, and BB' denotes the end of the link. Video-graphic data of the through movement was collected using a video camera mounted on a foot over bridge at the first location, and traffic signal post at the second location. For the first location, peak-hour traffic from 9 a.m. to 11 a.m. on July 2, 2018, was captured and seven signal cycles were identified for validation. At the second location, evening peak-hour traffic from 5 p.m. to 7 p.m. on February 14, 2020, was captured and five cycles were identified for validation. The timestamp and vehicle class of each vehicle crossing the

reference lines were extracted from the recorded video (Table 1). The vehicle composition for each cycle was then estimated in proportions (Table 1). The red duration and the signal cycle length for each cycle are determined from the video.

The vehicle composition at the study locations includes motorized two-wheelers, three-wheelers, four-wheelers, and heavy motor vehicles. From Table 1, it is evident that the composition and volume vary considerably during each cycle. It was observed that at both the locations, the two-wheeler proportion is the highest, and the four-wheelers constituted the second-highest

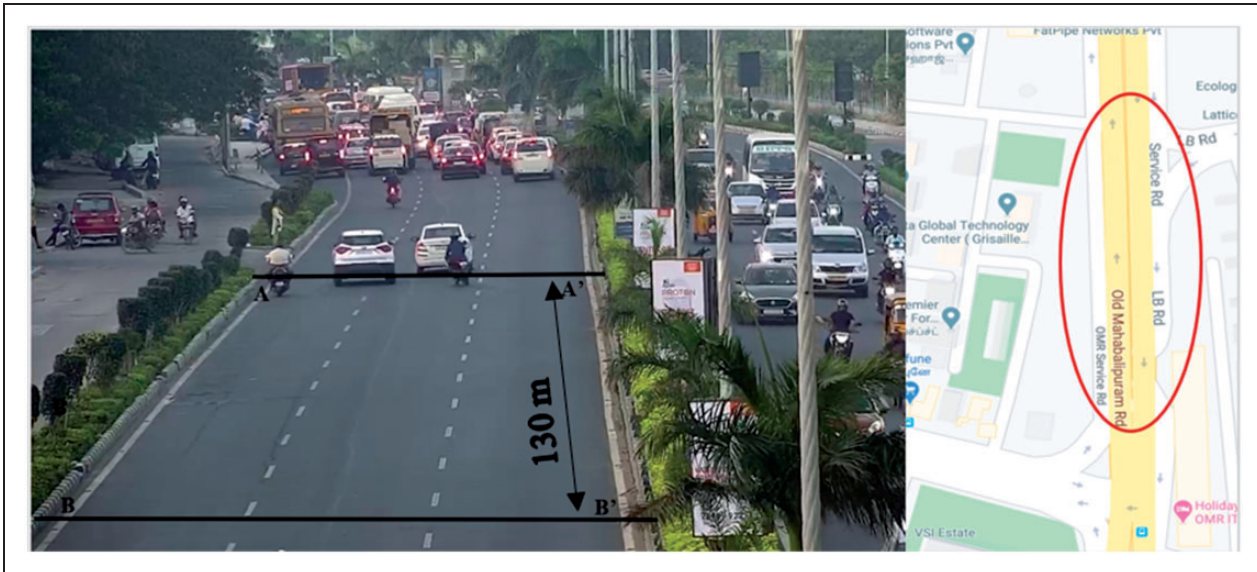


Figure 6. Study approach at the CSIR intersection, Chennai, India.

Table I. Signal Cycle Details with Traffic Volume and Composition

Location	Cycle	Total vehicles	Two-wheeler	Three-wheeler	Four-wheeler	Heavy motor vehicle	Red time (s)	Cycle time (s)
TIDEL Park intersection	1	79	82%	9%	5%	4%	230	355
	2	106	68%	8%	24%	1%	241	355
	3	132	54%	8%	36%	2%	274	386
	4	129	69%	7%	21%	3%	245	457
	5	132	70%	9%	17%	5%	202	340
	6	171	85%	4%	8%	4%	238	440
	7	181	90%	3%	4%	2%	277	433
CSIR intersection	1	94	50%	11%	35%	4%	137	201
	2	94	53%	6%	33%	7%	146	225
	3	96	55%	10%	29%	5%	139	209
	4	96	43%	8%	45%	4%	323	560
	5	80	46%	21%	18%	8%	52	93

proportion; in each cycle, three-wheelers and heavy vehicles together constituted less than 30%. With variation in the composition of vehicles across signal cycles, each signal cycle represents a different traffic condition, generally observed in the mixed traffic networks. Also, the red and cycle durations varied significantly across cycles (possibly operated by a police officer). The average red time observed was 244 s and 160 s at the TIDEL Park and CSIR location, respectively.

Estimation of Traffic Flow Parameters

The fundamental diagram parameters are estimated from the signalized intersection approaches to validate the link cost function and link capacity developed in this study. At each of the study locations, when the signal

turned red, the vehicles accumulated and filled the area between AA' and BB' (or sometimes spilled beyond BB'). When traffic turned green, vehicles begin to leave from AA' , and a queue relieving wave moved backward, and all the vehicles in the section $AA'-BB'$ left the site. Note that the link length is taken as $L = BB' - AA'$.

Jam density k_j is calculated as the total number of vehicles per kilometer occupying the section of road between AA' and BB' when the entire length L is filled with vehicles and are at the stopped condition.

Using the time stamp of all vehicle class data extracted at AA' , the cumulative count curve (N curve) is plotted as shown in Figure 7a, which represents the cumulative number of vehicles crossing the reference line. The figure also shows the oblique plot that explains the minor variation in the flow that will not be evident in

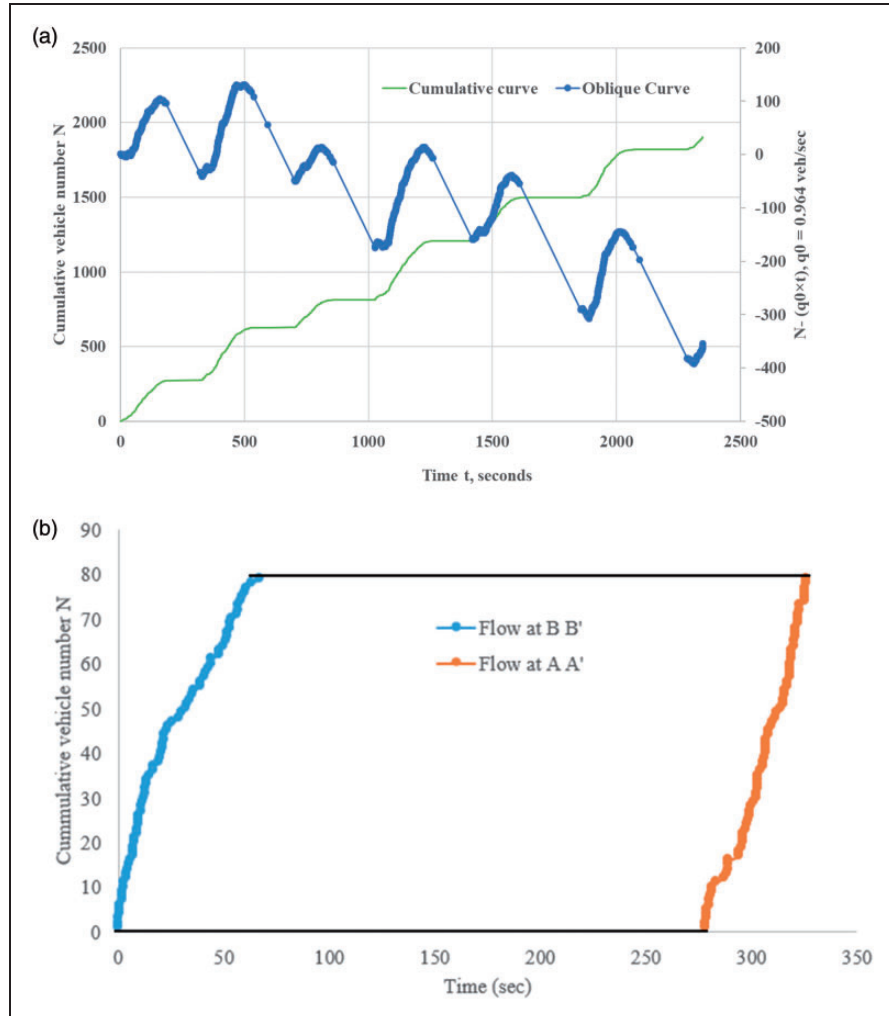


Figure 7. (a) Sample cumulative count and oblique curve at TIDEL Park intersection, and (b) N -curve for average travel time calculation.

the N -curves (26). It is derived using $N - (q_0 * t)$, where q_0 represents the average flow during the study period.

The average value of saturation flow is the positive slope on the N -curve from the time vehicles begin to leave AA' to the time vehicles from BB' arrive at AA' . Note that since the measurement starts not when the signal turns green, but when the vehicles at AA' begin to move, start-up loss time is already removed for the estimation of saturation flow.

The time taken t_1 by the shockwave to reach the reference line at BB' (upstream of the stop line) after the signal turns green is measured in each cycle. The wave speed is thus calculated as L divided by t_1 s. Finally, when the signal turns green, the critical speed, u_{cr} , at saturation flow is calculated using the time t_2 taken by the vehicles at BB' to reach AA' . Therefore, the critical speed is calculated as L divided by t_2 . Table 2 shows the jam density, saturation flow, wave speed, and the critical

speed at saturation flow measured during each signal cycle at the study sites.

It is clearly observed that the fundamental diagram parameters measured are dependent on the traffic state and composition. The cycles with a very high proportion of two-wheelers, like cycle 6 and cycle 7 of the first location, are observed to have a higher saturation flow rate. In non-lane-based mixed traffic conditions, vehicles tend to occupy any space available for them during jam conditions; two-wheelers especially fill the gaps available between larger vehicles. This, in turn, results in a higher saturation flow on green onset. Similarly, during the signal cycle 2 of TIDEL Park intersection and the last cycle of CSIR intersection, a higher proportion of heavy vehicles resulted in a lower value of jam density. This is because their higher lengths meant that the number of vehicles that could be accommodated in the stretch was lower. Also, these signal cycles (with a high

Table 2. Traffic Flow Parameters Measured at the Locations

Location	Cycle	Q (vph)	k_j (veh/km)	ω (km/hr)	u_{cr} (km/hr)
TIDEL Park intersection	1	4572	527	15.34	24.05
	2	5508	707	14.99	18.80
	3	7776	880	14.08	23.35
	4	6444	860	13.20	14.96
	5	6876	880	12.76	18.74
	6	9684	1140	14.44	20.91
	7	9360	1207	13.13	20.19
CSIR intersection	1	7345	723	17.62	23.99
	2	5947	723	17.74	27.05
	3	7391	738	16.40	25.67
	4	7528	738	16.55	26.55
	5	7786	615	15.96	23.60

Note: vph = vehicles per hour.

percentage of heavy vehicles) are observed to have higher wave speed compared with other cycles possibly because of larger vehicle lengths. With the increase in the proportions of fast-moving four-wheelers and two-wheelers, the stream speed generally increased.

Travel Time Data

The average travel time on a link is obtained from the area between the N -curves of the incoming and outgoing flows at AA' and BB' . As shown in Figure 7b, the area between the curves is divided by the total number of vehicles to obtain the average travel time on the link. It is assumed that the vehicles flow is first in, first out (FIFO) when the signal turns green and vehicles begin to move from the jammed state (this is a reasonable assumption, since all the vehicles are in a stopped condition during the jam condition and they begin to move when their turn comes).

With all the variables and the fundamental diagram parameters measured on the field, the next section presents an evaluation of the proposed link cost function and link capacity against the traditional models and empirical data.

Validation of Link Cost Function

During the study period, it was observed that the queue spilled beyond the section of length L under consideration. Therefore, the red time is scaled to the duration when the effect of the queue is observed in $BB'-AA'$, that is, the average of the stopped time spent by the first and the last vehicle in the queue.

Table 3 shows a comparison of the performance of the proposed models again the traditional models and empirical data. The empirical travel time is obtained as explained in the previous section. The BPR travel time values are calculated using the BPR function (Equation

1) with the assumed values of $\alpha=0.15$, $\beta=4$, and free-flow velocity, $u_f=40$ km/h, which is the speed limit on the study corridor (2). Similarly, the intersection delay values are obtained from the HCM delay model (Equation 2). The proposed link cost is calculated using Equation 9.

It is observed that the RMSE of combined “BPR function and HCM delay model” when compared with the empirical data was found to be 2.06 min. Moreover, it is found that the traditional function consistently underestimated the link cost for mixed traffic networks. However, the travel times obtained using the proposed cost function (Equation 9) are found to be closer to the empirical values. The average RMSE was found to be just 0.27 min. However, it was observed that the proposed function was sometimes overestimated or underestimated by small margins.

Next, the two terms of the proposed link cost (Equation 9) are evaluated separately. The first term is compared with the BPR function, and the second term is compared with the HCM delay model. Figure 8 shows a comparison of link travel time and intersection delay for the 12 cycles from two locations.

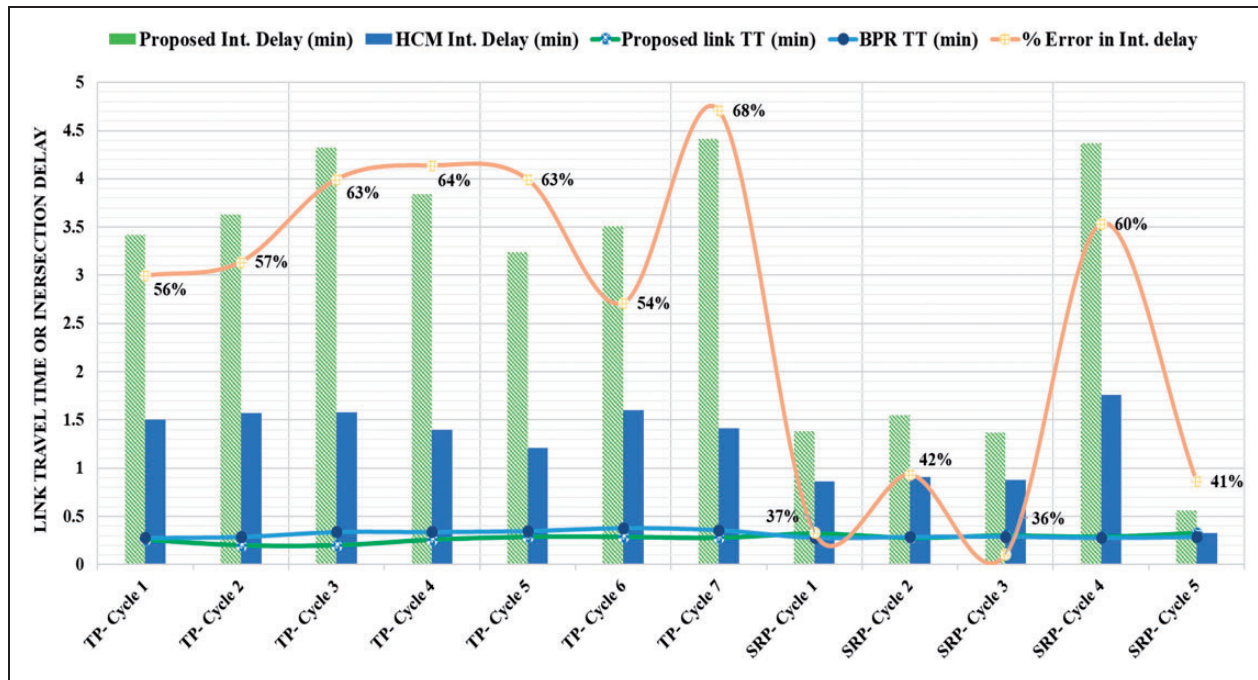
It is observed that the link travel times estimated by the proposed link cost function (Equation 9) appear very close to the values estimated by the BPR function, possibly because of the significantly lower magnitude of the link travel time compared with the intersection delay. In the mixed traffic urban networks, intersection delays are generally higher than link travel times because the traffic signal timings are often not optimized sufficiently and are manually controlled by traffic police or others during the peak periods. Lack of proper information to the police on the real-time traffic states on different approaches to the intersection often leads to longer reds and cycle lengths, resulting in sub-optimal signal operation. But the difference between BPR travel time

Table 3. Evaluation of Analytical Travel Time Data for 12 Signal Cycles

Location	Cycle	Empirical link cost* (min) (a)	BPR travel time + HCM delay (min) (b)	% error (a) and (b)	Proposed link cost* (min) (c)	% error (a) and (c)
TIDEL Park intersection	1	4.00	1.86	54%	3.83	4.0%
	2	3.94	1.78	55%	3.68	7.0%
	3	4.58	1.92	58%	4.52	1.0%
	4	4.22	1.74	59%	4.10	3.0%
	5	4.26	1.56	63%	3.53	17.0%
	6	4.06	1.98	51%	3.80	6.0%
	7	4.52	1.77	61%	4.69	-4.0%
CSIR intersection	1	1.65	1.15	31%	1.71	-3.6%
	2	1.73	1.20	31%	1.83	-5.8%
	3	1.72	1.17	32%	1.67	2.7%
	4	4.98	2.04	59%	4.66	6.4%
	5	0.88	0.62	30%	0.89	-1.1%

Note: BPR = Bureau of Public Roads; HCM = Highway Capacity Manual.

*Includes both link travel time and intersection delay.

**Figure 8.** Comparison of link travel time and intersection delay for 12 signal cycles.

Note: BPR = Bureau of Public Roads; HCM = Highway Capacity Manual; Int. Delay = intersection delay; SRP = SRP tools intersection; TT = travel time; TP = tidel park intersection.

and proposed link travel time may appear significant when the intersection delay is comparable with the link travel time.

Figure 8 shows that the proposed intersection delay values and the HCM delay equation differed significantly. The HCM delay model consistently underestimated the delay compared with the proposed intersection delay. The RMSE for the intersection delay comparison was

found to be 1.95 min. This shows that the proposed link cost function better represents the delay incurred in mixed traffic networks than the traditional models.

Validation of Link Capacity

The link capacity is empirically measured using the N -curves at BB' during the period from the time the first

Table 4. Empirical and Proposed Link Capacity during 12 Signal Cycles

Location	Cycle	Empirical link capacity (vph)	Proposed link capacity (vph)	% error
TIDEL Park intersection	1	4,293	3,884	9.5%
	2	7,252	3,939	45.7%
	3	6,260	3,842	38.6%
	4	4,698	3,979	15.3%
	5	6,095	4,753	22.0%
	6	4,752	3,009	36.7%
	7	4,650	3,997	14.0%
CSIR intersection	1	2,497	2,171	13.1%
	2	2,668	2,067	22.5%
	3	2,974	2,166	27.2%
	4	2,652	2,053	22.6%
	5	5,393	4,378	18.8%

Note: vph = vehicles per hour.

vehicles stops at the reference line AA' to the time the queue from AA' spills to BB' . The average flow of the N -curve is taken as the link capacity. Next, the proposed link capacity is estimated using Equation 14 using the field-observed parameters. Table 4 shows the empirical link capacity and the proposed link capacity observed at the two study locations.

Table 4 shows that the capacity values vary significantly across signal cycles depending on the vehicle class composition observed during that cycle; that is, cycles with higher (lower) proportion of smaller vehicles may have higher (lower) capacity values. Thus, variations in the empirical link capacity values confirm that a constant value for link capacity is not suitable for mixed traffic networks. It also shows that the proposed link capacity function gives variable capacity values for different cycles. The minimum error with the proposed model was found to be as low as 10%. However, sometimes it was higher, possibly because of the small duration of measurement (1 min), which may have resulted in the underestimation of jam density and saturation flow. Also, it was observed that the error was larger during the cycles with higher two-wheeler proportions indicating that locations with higher two-wheeler proportions may require validation using larger link lengths and measurement duration. Finally, it may be argued that, in the absence of any other suitable method in the literature, the proposed link cost and capacity functions are good candidates for representing mixed traffic conditions.

Conclusion

This study attempted to overcome the limitations of the traditional link cost function and link capacity identified in the literature by developing a novel link cost function in relation to link travel time and expression for link capacity in relation to vehicular traffic flow

suitable for mixed traffic networks with signalized intersections (delays at unsignalized intersections are not addressed in this paper). A comparison of empirical data against the traditional models and the proposed models shows that the proposed models perform significantly better than the traditional models for mixed traffic networks. The functions proposed are well-grounded on the existing theory of shock wave analysis and the parameters of the mixed traffic fundamental diagram.

Note that the impact of additional factors like curb friction, driver behavior, and so forth, commonly observed in mixed traffic networks, are also reflected in the newly developed functions, as these factors are latently incorporated in the fundamental diagram parameters for a given traffic composition on the link. It is expected that the results of this paper will immensely help the planning community in developing appropriate assignment models for effective planning and forecasting under mixed traffic conditions.

Acknowledgments

The authors thank the Ministry of Electronics and Information Technology (MeitY), Govt. of India, for supporting this research through the projects InTranSE-II - Departure Time Planner using V2V and V2I Communication and InTranSE-II—Development of a bus priority system at signalized intersection using V2I communication.

Author Contributions

The authors confirm contribution to the paper as follows: study conception and design: A. K. Das, B. Chilukuri; data collection: A. K. Das; analysis and interpretation of results: A. K. Das, B. Chilukuri; draft manuscript preparation: A. K. Das. All authors reviewed the results and approved the final version of the manuscript.

Declaration of Conflicting Interests

The author(s) declared no potential conflicts of interest with respect to the research, authorship, and/or publication of this article.

Funding

The author(s) disclosed receipt of the following financial support for the research, authorship, and/or publication of this article: The authors acknowledge the financial support from Tamil Nadu Road Development Company Ltd. in allowing us to instrument their corridor with traffic sensors.

References

1. Ambarwati, L., A. J. Pel, R. Verhaeghe, and B. van Arem. Empirical Analysis of Heterogeneous Traffic Flow and Calibration of Porous Flow Model. *Transportation Research Part C: Emerging Technologies*, Vol. 48, 2014, pp. 418–436.
2. Neuhold, R., and M. Fellendorf. Volume Delay Functions Based on Stochastic Capacity. *Transportation Research Record: Journal of the Transportation Research Board*, 2014. 2421: 93–102.
3. Huntsinger, L. F., and N. M. Rouphail. Bottleneck and Queuing Analysis: Calibrating Volume–Delay Functions of Travel Demand Models. *Transportation Research Record: Journal of the Transportation Research Board*, 2011. 2255: 117–124.
4. Khisty, C. J., and B. K. Lall. *Transportation Engineering an Introduction*. Prentice Hall, 1990.
5. Mtoi, E. T., and R. Moses. Calibration and Evaluation of Link Congestion Functions: Applying Intrinsic Sensitivity of Link Speed as a Practical Consideration to Heterogeneous Facility Types within Urban Network. *Journal of Transportation Technologies*, Vol. 4, No. 2, 2014, pp. 141–149.
6. Skabardonis, A., and R. Dowling. Improved Speed-Flow Relationships for Planning Applications. *Transportation Research Record: Journal of the Transportation Research Board*, 1997. 1572: 18–23.
7. Boyce, D. E., B. N. Janson, and R. W. Eash. The Effect on Equilibrium Trip Assignment of Different Link Congestion Functions. *Transportation Research Part A: General*, Vol. 15, No. 3, 1981, pp. 223–232.
8. Suh, S., C. H. Park, and T. J. Kim. A Highway Capacity Function in Korea: Measurement and Calibration. *Transportation Research Part A: General*, Vol. 24, No. 3, 1990, pp. 177–186.
9. Spiess, H..Technical Note — Conical Volume-Delay Functions. *Transportation Science*, Vol. 24, No. 2, 1990, pp. 153–158.
10. Nie, Y., H. M. Zhang, and D. H. Lee. Models and Algorithms for the Traffic Assignment Problem with Link Capacity Constraints. *Transportation Research Part B: Methodological*, Vol. 38, No. 4, 2004, pp. 285–312.
11. Branston, D. Link Capacity Functions: A Review. *Transportation Research*, Vol. 10, No. 4, 1976, pp. 223–236.
12. Manzo, S., O. A. Nielsen, and C. G. Prato. Investigating Uncertainty in BPR Formula Parameters: A Case Study. *Proc., Strateg Forsk i Transp og infrastruktur*, Danmarks Tekniske Universitet, 2013.
13. Rose, G., F. S. Koppelman, and M. S. Daskin. Analysis of the Effects of Parameter Estimation Error on Transportation Network Equilibrium Models. *Proc., International Symposium on the Theory of Traffic Flow and Transportation*, Berkeley, CA, 1987.
14. Aashtiani, H. Z., and H. Iravani. Use of Intersection Delay Functions to Improve Reliability of Traffic Assignment Model. *Proc., 14th Annual International EMME/2 Conference*, Chicago, IL, 1999, pp. 1–6.
15. Jeihani, M., S. Lawe, and J. P. Connolly. Improving Traffic Assignment Model using Intersection Delay Function. *Proc., 47th Annual Transportation Research Forum*, New York, N. Y., 2006.
16. Horowitz, A. J. Intersection Delay in Regionwide Traffic Assignment: Implications of 1994 Update of the Highway Capacity Manual. *Transportation Research Record: Journal of the Transportation Research Board*, 1997. 1572: 1–9.
17. Kurth, D. L., A. den Hout, and B. Ives. Implementation of Highway Capacity Manual-Based Volume-Delay Functions in Regional Traffic Assignment Process. *Transportation Research Record: Journal of the Transportation Research Board*, 1996. 1556: 27–36.
18. Koutsopoulos, H. N., and M. Habbal. Effect of Intersection Delay Modeling on the Performance of Traffic Equilibrium Models. *Transportation Research Part A: Policy and Practice*, Vol. 28, No. 2, 1994, pp. 133–149.
19. Larsson, T., and M. Patriksson. An Augmented Lagrangean Dual Algorithm for Link Capacity Side Constrained Traffic Assignment Problems. *Transportation Research Part B: Methodological*, Vol. 29, No. 6, 1995, pp. 433–455.
20. Dafermos SC. The Traffic Assignment Problem For Multiclass-User Transportation Networks. *Transportation Science*, Vol. 6, No. 1, 1972, pp. 73–87.
21. Lam, W. H. K., and H. J. Huang. A Combined Trip Distribution and Assignment Model for Multiple User Classes. *Transportation Research Part B: Methodological*, Vol. 26, No. 4, 1992, pp. 275–287.
22. Zhu, C., B. Jia, X. Li, and Z. Gao. A Stochastic Mixed Traffic Equilibrium Assignment Model Considering User Preferences. *Procedia-Social Behavioral Sciences*, Vol. 43, 2012, pp. 466–474.
23. Mesbah, M., M. Sarvi, and G. Currie. New Methodology for Optimizing Transit Priority at the Network Level. *Transportation Research Record: Journal of the Transportation Research Board*, 2008. 2089: 93–100.
24. Das, A. K., and B. R. Chilukuri. A Network Planning Approach for Truck Restriction in Heterogeneous Traffic. *Proc., 11th International Conference on Communication Systems & Networks (COMSNETS)*, Bengaluru, India, 2019, pp. 783–788.
25. May, A. D. *Traffic Flow Fundamentals*. Prentice-Hall, Englewood Cliffs, NJ, 1990.
26. Cassidy, M. J., and J. R. Windover. Methodology for Assessing Dynamics of Freeway Traffic Flow. *Transportation Research Record: Journal of the Transportation Research Board*, 1995. 1484: 73–79.